MULTITEMPORAL SAR DATA FOR URBAN CHANGE DETECTION USING MARKOV RANDOM FIELD: A CASE STUDY IN SHANGHAI

Osama Yousif[1] and Yifang Ban[2]

1. KTH Royal Institute of Technology, Division of Geoinformatics and Geodesy, Stockholm, Sweden; osama.yousif@abe.kth.se.
2. KTH Royal Institute of Technology, Division of Geoinformatics and Geodesy, Stockholm, Sweden; yifang@kth.se.

ABSTRACT

Multitemporal SAR images have been used increasingly in change detection analysis in the last few years. Most of the SAR images based change analysis, however, only considers per pixel information, thus ignoring the fact that, it is more likely for nearby pixels belonging to the same class, even though their intensity levels are different. Consequently, change detection algorithms that take into account textural and/or contextual information are desirable. Markov Random Field (MRF) has been used in the field of image classification and change detection to model pixels interdependencies into the analysis. Most of change detection studies that use SAR images in combination with MRF focused on the detection of single type of change either positive or negative change (e.g., flooded areas). Consequently, the change detection problem is addressed simply as a binary classification. In this research, our objective is to perform change detection analysis in urban areas where both positive and negative changes are expected. One bi-temporal dataset that covers Shanghai was used. The ratio operator is first used to construct a change image. Log normal density function is then used to model the distribution of the classes (unchanged, positive change, and negative change). The contextual information is used to model the prior probabilities and to reduce the effect of the speckle noise at the same time. Expectation maximization algorithm is used for the estimation of the unknown density functions parameters. The best detection accuracy at 81% was achieved using the MRF-based algorithm compared to 75% when using Kittler-Illingworth double thresholding algorithm.

INTRODUCTION

Change detection using multitemporal remote sensing images is indispensable tools for many applications. Deforestation, forest fire, desertification, flooding, urban sprawl, disaster monitoring and damage assessment are some of the possible area of applications (e.g., 1, 2, 3). The low cost, large coverage and accessibility are among the reasons for the use of remote sensing images in change detection analysis. However, to extract useful change information from these images, many problems have to be addressed. The uncertainty of the measured phenomena itself, negative effects of the atmosphere, and speckle effects in SAR image, are among the issues that should be treated carefully when dealing with change detection analysis. Over the years, many change detection algorithms have been developed that have focused in different aspect of the problem (e.g., 1, 2, 3, 4).

Recently, increasing attention has been paid to the preservation of spatial details and structures when performing classification or change detection analysis. This is particularly important when the intention is to detect urban changes using SAR images with speckles. In (4) the problem of details conservation is tackled by using wavelet transform to decompose the change variable into many scale-dependent images. For classification of each pixel, a suitable scale is decided based on the evaluation of global and local statistics. Markov random field (MRF) has also been used to maintain details in image classification and change detection. MRF is an efficient tool to model contextual information in image analysis. Its flexibility increases its use in image classification (5, 6, 7, 8), and image segmentation (9).

MRF has also been used in the field of change detection (12, 13, 14). In (15), a SAR-specific extension of Fisher transform combined with expectation maximization (EM) algorithm is used to automatically extract change information from a multichannel, multitemporal SAR images. In (16), an unsupervised change detection algorithm that exploits multichannel-multitemporal SAR images has been developed. There, MRF was used to model the contextual component, and to provide a framework for data-fusion. For SAR image classification or change detection, besides modeling pixels interdependencies, MRF can play an important role in reducing the effect of speckles (15, 16). In this study, our objective is to identify changes in urban areas using MRF-based change detection algorithm. Urban changes are usually characterized by both intensity increase (positive change) and intensity decrease (negative change) over time. Furthermore, changes normally occurred in small discrete patches distributed all over the study area. Using MRF-based change detection algorithm can help in detecting these changed areas and preserving spatial structure and details at the same time.

METHODOLOGY

The first step in change detection analysis is the generation of change image by comparing the multitemporal images. For SAR images, the ratio operator is normally preferred since it helps in reducing the effect of the multiplicative speckle (4). Assuming two co-registered SAR images I_1 and I_2, of size $R \times C$ acquired at time t_1 and t_2 respectively, then the change image R can generated by dividing the first date image I_1 by the second date image I_2 in a pixel by pixel basis.Change in urban areas, as measured in SAR images, is normally characterized by intensity decrease or intensity increase. Hence, in this study our change variable R is considered to be a combination of three different classes, unchanged (ω_{uc}), positive change (ω_{pc}), and negative change (ω_{nc}).

Given the change variable R, the objective is to generate a change map Ω in which each pixel $\Omega_{r,c}$ can only assumes a value from the label domain ω: $\{\omega_{uc},\omega_{pc},\omega_{nc}\}$. According to Bayesian theory, the optimum label $\Omega_{r,c}$ of the pixel at location (c,r), is the one that maximizes the posterior probability or minimizes its equivalent energy representation as shown in Eq. 1.

$$\Omega_{r,c} = \arg\min_{\omega_i \in \omega} \{-\ln[p(R_{r,c} / \omega_i)] - \ln[P(\omega_i)]\} \quad (1)$$

Where, $p(R_{r,c}/\omega_i)$ is the probability of $R_{r,c}$ conditioned to class ω_i, and $P(\omega_i)$ is the prior probability of class ω_i. MRF presents a way to model the prior probability using local contextual information. It is based on the assumption that, the labels configuration Ω represents a Markov random field. Then, based on the equivalency of MRF and Gibbs random field, and using pair-site MRF model (Ising model), the prior probability component in Eq. 1 can be modelled locally using labels configuration in a defined neighbourhood system N (Eq. 2).

$$\ln[P(\omega_i)] = \ln[P(\omega_i / N_{r,c})] = \beta \frac{m_{r,c}}{n} \quad (2)$$

Where $m_{r,c}$ is the number pixels having a label equal to ω_i in the neighbourhood of pixel (r,c), and n indicates the total number of pixels in the neighbourhood system N (10). The contextual parameter β, known also as the attraction parameter (11), controls the contribution of the contextual component in the classification process.

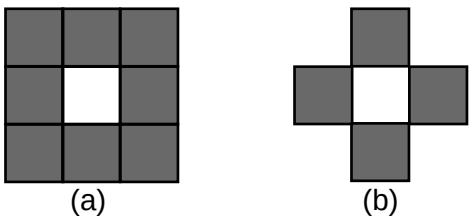

Figure 1: (a) first order neighborhood, and (b) second order neighborhood.

Log normal distribution has been widely accepted as a heuristic density model that can be used to describe the statistics of amplitude/intensity SAR images. Additionally, it has been found that this model can also be used to describe the statistical behavior of the change and unchanged classes as examined in the ratio of SAR images (16). Consequently, this density function will be used to describe the statistics of the classes as examined in the change image. The parametric form of the log normal distribution is shown in Eq. 3.

$$p(R/\omega_i) = p(R/\mu_i, \sigma_i^2) = \frac{1}{R\sigma_i\sqrt{2\pi}} \exp\left[-\frac{(\ln R - \mu_i)^2}{2\sigma_i^2}\right] \quad (3)$$

Where μ_i and σ_i^2, are the mean and variance of the associated normal distribution and i refers to one of the three classes $\{\omega_{uc}, \omega_{pc}, \omega_{nc}\}$.

Eq. 1 is solved iteratively where at each cycle the samples assigned to each class are used to make a new estimation of the class's density function parameters. A fast EM algorithm developed in (5) is used for the estimation of the PDFs parameters, in which the samples are weighted by their current posterior probabilities. The current change map is used to locally model the prior probability (Eq. 2). A new change map is then generated using Eq. 1. The iteration continues until the PDFs parameters converge.

The MRF-based change detection formulated in Eq. 1 has two requirements. First, the neighbourhood system N must be defined in advance. In this research, two types of neighbourhood configuration were tested, i.e., first order, and second order neighbourhood in Fig. 1 (a) and (b) respectively. Second, the application of MRF-based change detection algorithm requires an initial change map. To generate this change map, Kittler-Illingworth double thresholding algorithm (KIDT) will be used (17). This algorithm uses histogram fitting technique to automatically locate two thresholds to separate the three classes (unchanged, positive change, and negative change). Log normal distribution is utilized to model the statistics of the classes. KIDT is sensitive to the existence of speckles. Consequently, a despeckling phase using Gamma MAP filter was necessary.

DATA DESCRIPTION

To test the efficiency of the algorithm multitemporal SAR datasets was used. The experiment dataset covers the south-eastern part of Shanghai city, and includes one ERS-2 SAR scene from Sep 7, 1999, and ENVISAT ASAR scene from Sep 19, 2008. Fig. 3 (a) shows Shanghai change variable produced by applying the ratio operator to multitemporal SAR images. The SAR images were acquired in near anniversary dates to eliminate seasonal effects and consequently avoiding the detection of spurious changes. To quantitatively assess the quality of the final change map, 1657 changed and 1663 unchanged pixels have been used.

RESULTS AND DISCUSSION

The initial change results including the false alarm, detection accuracy, and Kappa coefficient are presented in Table 1. It is obvious that, KIDT achieve a low false alarm rate. However, the detection accuracy is low. This low quality change map can be attributed to the fact that, KIDT is sensitive to the existence of more than three modes in the histogram of the ratio image.

The MRF-based change detection algorithm is applied to the unfiltered SAR images. Higher value of the contextual parameter β will lead to over smoothed change map while smaller value will produce a noisy one. In this study, different values of β [2, 3…7] has been tested for both the 1st and 2nd order neighborhoods. Fig. 2 shows the variation of Kappa coefficient as function of β. As the figure indicates, 1st and 2nd order neighborhoods perform equally well, with slight improvement when using the latter one. Additionally, the figure indicates that, the kappa curve peaks at β=4.

Table 1: Accuracy assessment (Shanghai).

		False Alarm	Detection Accuracy	kappa Coefficient	NO of Iterations
KIDT		2.16	75.26	73.12	
β=2	N_1	27.12	90.28	63.14	46
	N_2	36.44	92.21	55.75	67
β=3	N_1	5.65	83.77	78.13	27
	N_2	5.83	83.28	77.47	26
β=4	N_1	2.10	80.45	78.37	21
	N_2	2.04	81.05	79.03	20
β=5	N_1	1.56	79.12	77.58	11
	N_2	1.32	79.06	77.76	12
β=6	N_1	1.62	78.03	76.44	8
	N_2	1.14	76.64	75.53	11
β=7	N_1	1.62	77.43	75.83	6
	N_2	1.08	76.58	75.53	11

Fig. 3 shows the ratio image (a), KIDT-based change map (b), MRF-based change map using 1st order neighborhood (c), and 2nd order neighborhood (d). The positive change is shown in blue, while the negative change is shown in red. Observing these figures, one can realize that KIDT-based change map miss many of small changed areas. Moreover, the adaptive filter, although important for reducing speckle, reduces the amount of spatial details available in the original change image. On the other hand, MRF-based change detection algorithm, either 1st or 2nd order neighborhood manages to identify most of small changed areas. The area highlighted with yellow circle in Fig. 3 shows part of Shanghai's airport. In this area there are a many small unchanged patches located between the runways in Fig. 3 (a). Using adaptive filter before applying KIDT algorithm causes these small unchanged regions to be erroneously identified as changed in Fig. 3 (b). On the other hand MRF-based change detection algorithm, managed to correctly identifies these region as unchanged Fig. 3 (c) and (d).

Finally, Table 1 shows the accuracy assessment of Shanghai change maps produced using different values of Beta under 1st (N1) and 2nd (N2) order neighborhoods. The best results were obtained when β=4, and the results obtained under the 2nd order neighborhood are in general slightly better than those obtained using the 1st order neighborhood. From the table, it is also obvious that MRF-based change detection algorithm managed to significantly improve the detection accuracy regardless of the quality of the initial change map.

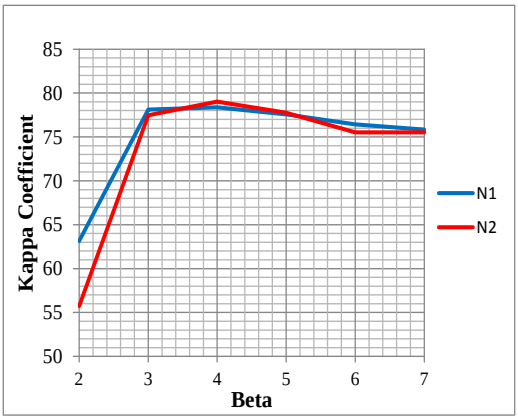

Figure 2: Kappa coefficient of agreement as function of Beta.

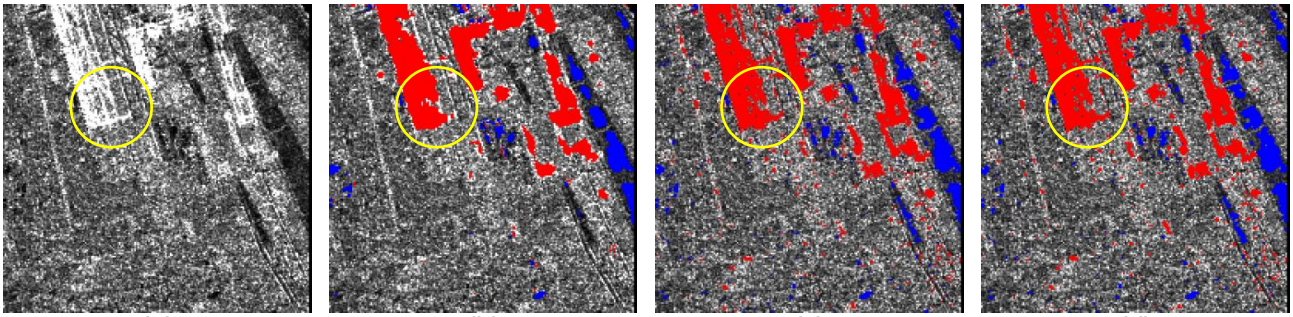

(a) (b) (c) (d)

Figure 3: (a) change image, (b) Change map produced using KIDT, (c) Change map produced using MRF with 1st order neighborhood, and (d) Change map produced using MRF with 2nd order neighborhood (blue: positive change, and red: negative change).

CONCLUSION

Change detection in urban areas using multitemporal SAR images present huge challenges. These changes are normally consists of small discrete patches that can be either positive or negative. The existence of the speckles further complicates the analysis. MRF-based change detection algorithm can play important role in this context. Owing to its ability to model pixels interdependencies, to suppress the negative effect of speckles, and to preserve the spatial details, MRF has significantly improved the change detection accuracies in urban areas. First order and second order neighborhood perform equally well for both dataset. Although, the 2nd neighborhood achieved slight better detection accuracy and less noisy change map.

Although MRF-based change detection algorithm achieved good detection accuracies in urban environment, there is still room for further improvements. First, only one PDF (log normal) has been considered so far. The result can be improved by considering other density functions (Weibull ratio, generalized Gaussian…etc.). Second, enhancement can also be achieved by the addition of another layer of information to the change image. One example is the addition of a linear enhanced image derived from the change variable that accentuates linear features and objects edges. Fusion of information from these layers in addition to the contextual component will hopefully lead to better detection accuracies.

ACKNOWLEDGEMENT

This research was supported by the Swedish National Space Board. The research is also part of the project ‘Satellite Monitoring of Urbanization for Sustainable Urban Development’ within the European Space Agency (ESA) and Chinese Ministry of Science and Technology (MOST)’s Dragon II program. The authors would like to thank ESA for the ENVISAT and ERS-2 SAR data.

REFERENCES

1. Ban, Y. and Yousif, O., ‘Multitemporal Spaceborne SAR Data for Urban Change Detection in China. IEEE Journal on Selected Topics in Applied Earth Observations and Remote Sensing (In Press), 2012.
2. Martinis, S., Twele, A., and Voigt, S., ‘Unsupervised Extraction of Flood-Induced Backscatter Changes in SAR Data Using Markov Image Modeling on Irregular Graphs’, IEEE Transactions on Geoscience and Remote Sensing, Vol. 49, NO. 1, pp. 251-263, 2011.
3. Gamba, P., F. Dell'Acqua, and Trianni, G., ‘Rapid Damage Detection in the Bam Area Using Multitemporal SAR and Exploiting Ancillary Data’, IEEE Transactions on Geoscience and Remote Sensing, Vol. 45, NO. 6, pp. 1582-1589, 2007.

4. Bovolo, F., and Bruzzone, L., 'An Adaptive Multiscale Approach to Unsupervised Change Detection in Multitemporal SAR Images', IEEE International Conference on Image Processing, ICIP, 2005.
5. Jackson, Q., & Landgrebe, D. A., 'Adaptive Bayesian Contextual Classification Based on Markov Random Fields', IEEE Transactions on Geoscience and Remote Sensing, Vol. 47, NO. 11, pp. 2454-2463, 2002.
6. Tso, B. C. K., and Mather, P. M., 'Classification of Multisource Remote Sensing Imagery Using a Genetic Algorithm and Markov Random Fields', IEEE Transactions on Geoscience and Remote Sensing, Vol. 34, NO. 3, pp. 1255-1260, 1999.
7. Solberg, A. H. S., Taxt, T., and Jain, A. K., 'A Markov Random Field Model for Classification of Multisource Satellite Imagery', IEEE Transactions on Geoscience and Remote Sensing, Vol. 34, NO. 1, pp. 100-113, 1996.
8. Melgani, F., and Serpico, S. B., 'A Markov Random Field Approach to Spatio-Temporal Contextual Image Classification', IEEE Transactions on Geoscience and Remote Sensing, Vol. 41, NO. 11, pp. 2478-2487, 2003.
9. Deng, H., and Clausi, D. A., 'Unsupervised image segmentation using a simple MRF model with a new implementation scheme', Pattern Recognition Vol. 37, pp. 2323 – 2335, 2004.
10. Grazelli, A., 'Classification of polarimetric SAR images using adaptive neighborhood structures', International journal of Remote Sensing, Vol. 20, NO. 8, pp. 1669-1675, 1999.
11. Smits, P. C., and Dellepiane, S. G., 'Synthetic Aperture Radar Image Segmentation by a Detail Preserving Markov Random Field Approach', IEEE Transactions on Geoscience and Remote Sensing, Vol. 35, NO. 4, pp. 844-857, 1997.
12. Kasetkasem, T., and Varshney, P. K., 'An Image Change Detection Algorithm Based on Markov Random Field Models', IEEE Transactions on Geoscience and Remote Sensing, Vol. 40, NO. 8, pp. 1815-18263, 2002.
13. Bruzzone, L., and Prieto, D. F., 'Automatic Analysis of the Difference Image for Unsupervised Change Detection', IEEE Transactions on Geoscience and Remote Sensing, Vol. 38, NO. 3, pp. 1171-1182, 2000.
14. Bruzzone, L., and Prieto, D. F., 'An Adaptive Semiparametric and Context-Based Approach to Unsupervised Change Detection in Multitemporal Remote-Sensing Images', IEEE Transactions on Geoscience and Remote Sensing, Vol. 11, NO. 4, pp. 452-466, 2002.
15. Moser, G., and Serpico, S. B., 'Unsupervised Change Detection From Multichannel SAR Images', IEEE Transactions on Geoscience and Remote Sensing, Vol. 4, NO. 2, pp. 278-282, 2009.
16. Moser, G., and Serpico, S. B., 'Unsupervised Change Detection from Multichannel SAR Data by Markovian Data Fusion', IEEE Transactions on Geoscience and Remote Sensing, Vol. 47, NO. 7, pp. 2114-2128, 2009.
17. Bazi, Y., Bruzzone, L., and Melgani, F., 'Automatic Identification of the Number and Values of Decision Thresholds in the Log-Ratio Image for Change Detection in SAR Images', IEEE Transactions on Geoscience and Remote Sensing, Vol. 3, NO. 3, pp. 349-353, 2006.